NASA TM-1998-207913

Development of Algorithms and Error Analyses for the Short Baseline Lightning Detection and Ranging System

Stan Starr
Dynacs Engineering Co., Inc.
John F. Kennedy Space Center, Florida

National Aeronautics and Space Administration
John F. Kennedy Space Center, Kennedy Space Center, Florida 32899-0001

August 1998

ABSTRACT

NASA, at the John F. Kennedy Space Center (KSC), developed and operates a unique high-precision lightning location system to provide lightning-related weather warnings. These warnings are used to stop lightning-sensitive operations such as space vehicle launches and ground operations where equipment and personnel are at risk. The data is provided to the Range Weather Operations (45th Weather Squadron, U. S. Air Force) where it is used with other meteorological data to issue weather advisories and warnings for Cape Canaveral Air Station and KSC operations. This system, called Lightning Detection and Ranging (LDAR), provides users with a graphical display in three dimensions of 66 megahertz radio frequency events generated by lightning processes. The locations of these events provide a sound basis for the prediction of lightning hazards. This document provides the basis for the design approach and data analysis for a system of radio frequency receivers to provide azimuth and elevation data for lightning pulses detected simultaneously by the LDAR system. The intent is for this direction-finding system to correct and augment the data provided by LDAR and, thereby, increase the rate of valid data and to correct or discard any invalid data. This document develops the necessary equations and algorithms, identifies sources of systematic errors and means to correct them, and analyzes the algorithms for random error. This data analysis approach is not found in the existing literature and was developed to facilitate the operation of this Short Baseline LDAR (SBLDAR). These algorithms may also be useful for other direction-finding systems using radio pulses or ultrasonic pulse data.

ACKNOWLEDGEMENTS

The author would like to thank the following individuals for their contributions to this work. First, thanks to both the KSC Weather Office (John Madura and Dr. Frank Merceret) and the KSC Technology Programs and Commercialization Office (especially David Makufka, Joni Richards, and Jim Aliberti) for sponsoring the development of the Short Baseline LDAR System. Thanks to Steve Boyd of the Engineering Development Directorate for coordinating and directing all the LDAR projects, including this one. Thanks to Carl Lennon for conceiving the SBLDAR system and providing continuous moral and technical support throughout its development. Thanks to Mike Brooks who performed or coordinated the physical build up of the system including trenching, computer setup, programming, algorithm testing, and, perhaps most important of all, establishing the array geometry. Thanks to Bradley Burns for his many contributions to Mike's work and his own accomplishments in the setup, conceptual development, and testing of the SBLDAR. Mike and Bradley also very carefully reviewed this work and provided many corrections and clarifications. Thanks also to Anne Roseberry and Jane Flynn for careful and insightful review and editing. Thanks to Dr. Robert Youngquist and Dr. Pedro Medelius for many stimulating conversations regarding lightning physics and location math. Thanks to Caroline Zaffery for the great illustrations. Greatest thanks to Michele Athman for a tremendous job of typing and editing, but most of all for her patience and perseverance.

TABLE OF CONTENTS

ABBREVIATIONS AND ACRONYMS

AZ	azimuth
AZDOP	azimuth dilution of precision
c	speed of light (0.2997 meters/nanosecond)
CCAS	Cape Canaveral Air Station
cm	centimeter
cos	cosine
$\cos^{-1}$	arc cosine
CRC	Chemical Rubber Company
DOP	dilution of precision
DTOA	difference of time of arrival
EL	elevation
ELDOP	elevation dilution of precision
ER	Eastern Range
FIFO	first-in-first-out
FM	frequency modulation
GHz	gigahertz
km	kilometer
KSC	John F. Kennedy Space Center
l	length of baseline (meters)
LDAR	Lightning Detection and Ranging
LLP	Lightning Location and Protection
log	logarithm, base 10
MHz	megahertz
NASA	National Aeronautics and Space Administration
NLDN	National Lightning Detection Network
NOAA	National Oceanic and Atmospheric Administration
ns	nanosecond
ONERA	Office National D'Etudes et de Reserches Aerospatiales
RF	radio frequency
rms	root mean square
SBLDAR	Short Baseline Lightning Detection and Ranging
SGN	sign function, equal to + or -
sin	sine
$\sin^{-1}$	arc sine
tan	tangent
$\tan^{-1}$	arc tangent
TOA	time of arrival
USAF	United States Air Force
VHF	very high frequency

σ	standard deviation
3-D	three-dimensional
π	pi, the ratio of the circumference to the diameter of a circle

1. INTRODUCTION

1.1 BACKGROUND

John F. Kennedy Space Center (KSC) operations emphasize safety. The combination of Florida's frequent thunderstorms and the hazardous and expensive equipment involved in space flight operations requires strict attention to lightning hazards. Lightning can ignite propellants, induce damaging voltages and currents in critical circuitry, and injure or kill personnel. KSC and the United States Air Force (USAF) Eastern Range (ER) have experienced significant lightning-induced system failures including the double lightning strike to the Apollo 12 Saturn V launch vehicle, which almost aborted the second moon landing mission in 1969 [1, 2 ,3]; significant damage to the Viking 1 orbiter spacecraft while inside a processing facility in 1975 [4]; and the triggered strike to and subsequent loss of the Atlas Centaur AC-67 launch vehicle in 1987 [5]. As a result of these and other experiences, a major emphasis is placed on proper facility protection, the real-time monitoring of lightning hazards, and the cessation of sensitive operations when lightning activity occurs in the vicinity. These safety rules [6] require systems capable of measuring atmospheric electrical potentials and accurately locating lightning events.

Lightning and clouds posing the threat of lightning in the KSC/Cape Canaveral Air Station (CCAS) area are monitored using six separate systems: "field mill" network that measures atmospheric electric potential gradients near the ground, the National Lightning Detection Network (NLDN), a local equivalent of NLDN called Lightning Location and Protection (LLP), a 5-centimeter (cm) weather radar (WSR-74C), a 10-cm Doppler weather radar (WSR-88D), and the Lightning Detection and Ranging (LDAR) System for locating and displaying radio pulses produced by lightning events. Based on input from these systems, especially LDAR, KSC lightning safety policy dictates that personnel be warned of lightning events occurring near the KSC area and that specific operational and personnel controls be established when lightning is detected within 5 miles of an operational area [6].

KSC developed and operates the LDAR system, which receives and detects radio pulses emitted during lightning events and locates each pulse in local east, north, and height (x, y, z) coordinates. It operates on the principle of hyperbolic position location. In this scheme, the difference of time of arrival (DTOA) of a signal received by two separated radio receivers indicates that the source lies on a hyperbolic cone centered on the baseline joining the two receivers. A hyperbola is defined as a curve that, for any point on the curve, the difference in distances between that point and two fixed foci is a constant. This constant is the difference in times of arrival multiplied by the speed of light. The system establishes a number of baselines, each one producing a hyperbolic cone; the intersection of these cones gives the estimated position of the source.

LDAR was developed by Carl Lennon, a former NASA engineer, and others in the mid-1970's, to support lightning research activities in the KSC area. The LDAR system was upgraded several times to support research objectives and came to be unofficially relied upon to determine lightning risks to KSC operations. In the early 1990's, Mr. Lennon, Launa Maier, and others established the LDAR system as operational, and it has become an integral part of the weather warning system at KSC and CCAS. A more complete description of the LDAR system is available in references 7 and 8.

The LDAR system has seven very high frequency (VHF) radio receivers, one at the central site and six on a roughly 10-kilometer (km) circle. The receivers operate at 66 megahertz (MHz) with a bandwidth of about 6 MHz. The receivers form two Y-shaped arrays laid on top of each other in opposite orientations forming a star shape. Each remote site includes an LDAR receiving antenna, a logarithmic amplifier, and a 4-gigahertz (GHz) microwave line-of-site link back to the central site. The log amp results in a much higher dynamic range but also minimizes amplitude differences and rectifies the signal (i.e., all signal values are positive with no zero crossings). At a preestablished signal level, the central channel triggers a recording of 81.92 microseconds of data from all seven channels. Each data stream is sampled at 100 MHz with 8-bit resolution. The peak amplitude time tag is determined from each channel and corrected for the known time delay due to the microwave transmission link. The time of arrival from each remote site is subtracted from that of the central and used to form two solutions of location, one for each Y-shaped array. If the horizontal range for two solutions agrees to within 0.35 km when the determined range is less than 7 km and otherwise agrees to within 5 percent of the horizontal range, the solution is declared valid. If not, a voting procedure involving all 20 combinations of sites is implemented involving comparison of the horizontal range solutions. If at least seven of the combinations agree to within the above stated limits, the solution is declared valid.

The LDAR system is very useful to KSC and ER meteorologists in providing graphical displays of recently recorded valid events. These displays, when used in conjunction with radar images of precipitation and other information sources, provide excellent warnings of possible lightning hazards in operational areas. Unfortunately, some 60 percent of all system triggers result in discarded solutions. In addition, the possibility for false solutions exists such that events are plotted at the correct range but with azimuth error of 180 degrees. The sources of these errors in the LDAR solutions are believed to include:

a. The use of peak value rather than waveform matching to determine DTOA's.

b. The change in order in time of events measured at widely separated locations.

c. The nonisotropic emission of radio waves from sources resulting in wide variations in intensity at different locations.

d. The nonlinear nature of LDAR equations resulting in occasional sign errors in X and Y coordinates.

Discarded events and incorrectly placed events can result in shutting down operations unnecessarily, wasting valuable resources, or the underestimation of lightning hazards.

Carl Lennon conceived of a solution to augment the LDAR system with a short baseline version of LDAR located near the central site, which would reliably provide azimuth (AZ) and elevation (EL) data to validate and perhaps correct both false solutions and failed solutions. This system is called Short Baseline LDAR (SBLDAR).

1.2 SBLDAR SYSTEM DESCRIPTION

The SBLDAR system is a radio direction-finding system intended to augment the existing LDAR system. The SBLDAR system consists of six antennas, four in a "Y" pattern in the local horizontal plane and two mounted on a tower one above the other. Radio signals received by the antennas over a frequency band from roughly 25 to 250 MHz are recorded using high-speed transient digitizers that are triggered at the same moment the operational LDAR system triggers. The data is high pass filtered at 25 MHz to eliminate low-frequency noise, notch filtered in the frequency modulation (FM) radio broadcast band to eliminate radio and television interference, and low-pass filtered at 250 MHz to eliminate aliasing. The data records in the prototype system are only 2 microseconds long but are sampled at 500 MHz. Each data record is cross correlated with the others. The peak of the cross correlation function is curve fit with a polynomial to enhance the estimation of the DTOA. The DTOA's are used to form an estimate of the AZ and EL of the lightning source. This AZ and EL estimate may be used to efficiently filter out erroneous LDAR solutions for the matching lightning events or may be used to improve the accuracy of the LDAR solution.

This document develops the necessary equations to analyze DTOA data to determine AZ and EL using arrays like the SBLDAR. It does not address the process of analyzing the data to estimate the DTOA's themselves.

1.3 SBLDAR COMPARED TO OTHER RADIO FREQUENCY (RF) AND LIGHTNING LOCATION SYSTEMS

It may be surprising that algorithms and analyses would need to be developed in a field as mature as radio direction finding. This section places the SBLDAR system in the context of this field.

RF direction-finding systems can be categorized by the manner in which they interact with the incoming radiation to derive a direction. For sources that are continuous in time and in which the radiated energy has a narrow spectral distribution, direction-finding systems can utilize the interference of waves from the source. Detectors can be spaced at less than one wavelength and their received phase compared. These types of systems are called interferometers, although many do not directly add the received waves together vectorally. Directional ambiguities can be resolved by adding detector rows at right angles and by adding additional arrays at different spacings. The mathematics of these types of receivers is well established and continues to be an active field. Applications of direction finding for narrow band continuous sources include electronic warfare, radio navigation, radio astronomy, and, more recently, cellular phone reception enhancement. For recent reviews of the field, see references 9 and 10.

Interferometers have also been used to provide the direction to lightning radio sources. A French organization, the Office National D'Etudes et de Reserches Aerospatiales (ONERA), has provided the National Oceanic and Atmospheric Administration (NOAA), with a VHF interferometer lightning radio mapping system. This system includes a station that operates on the grounds of KSC not far from the location of the LDAR central site. The system works by using multiple antennas along a single (azimuth only) or multiple (azimuth and elevation) baselines. The signals received by pairs of antennae are narrow band filtered (so they can interfere) then quadrature summed to derive a relative phase. This phase difference is a function of the wavelength (provided by the speed of light divided by the center frequency) and the spacing of the antennae in wavelengths. By having two such baselines at different wavelength spacings, an integer number of wavelengths can be eliminated so the phase residual depends only on the angles of azimuth and elevation. These systems are described in references 11, 12, and 13. They are very similar to the Short Baseline LDAR in that they derive angle-only data. Range must be provided by using multiple systems with overlapping sensitive areas. Lightning interferometers suffer from numerous false locations at the actual azimuth plus 90, 180, and 270 degrees. Because the ONERA-3D system is a research system, not a real-time warning system, an operator can pick through the data, eliminating false data. As stated in reference 11, which compared KSC LDAR and the ONERA 3D System:

> "...the TOA system [LDAR] (1) is best suited for mapping the individual, spaced pulses of short duration (a few microseconds long) in a low rate radiation process, (2) resolves pulses separated in space and occurring in time intervals greater than the data window, but (3) cannot discern individual pulses in noise-like Q trains. The ITF system [ONERA-3D] (1) is better suited for mapping the Q train sequences (characterized by continuity of phase), but (2) cannot resolve two simultaneous continuing radiation processes separated in space (e.g., two Q train sequences or one Q train and a discontinuous sequence of pulses)."

Note that Q trains are semicontinuous noise like RF lightning signals.

Time-of-arrival (TOA) systems include radar and LDAR. In radar, the operator originates the radiated pulse so reflected pulse structure and timing is available. LDAR is somewhat like passive bistatic radar, wherein an eavesdropper listens to pulses reflected from targets without knowledge of the original pulse shape or timing. Systems based on uncontrolled pulsed sources typically use hyperbolic positioning like LDAR because the time of signal start is not available. A considerable amount of mathematics has been developed to perform passive hyperbolic positioning, but most is based on tracking moving sources where some assumptions about target dynamics can be assumed (e.g., aircraft flying on straight course) and multiple data points are available through repetition. For example, locating a downed flyer by using a pulsed transmitter applies knowledge of the search aircraft motion and the assumption that the emitter is not moving. Applicable and excellent general references on the problems of these hyperbolic location systems include references 14 and 15.

LDAR receives only a single pulse or pulse train per event. Systems of this type must rely on maximizing the information available from the single isolated event recorded at multiple stations. The design approach of such systems can be partitioned into two areas: the means for estimating the DTOA's (including antenna design, filtering, digitizing, data storage, and differencing) and the algorithm approach to the determination of position. The algorithms available for hyperbolic positioning involve solving for points in x, y, and z that are common to multiple hyperbolic cones. These approaches typically take the form of a pseudolinear algebraic approach. All eventually boil down to solving for the roots of several simultaneous equations. Several schemes have been conceived to perform this function, the best of which is probably that used by the LDAR system. Most of the approaches in the literature are not capable of operating in cases where all the detectors lie in a plane such as with LDAR and SBLDAR unless the source is confined to the same plane. All the approaches found in our research, except LDAR's, are iterative approaches, involving searching for these roots. These algorithms are evaluated and compared in the literature based on the time required to locate these roots and the probability that the incorrect root or solution will be selected. Since LDAR is a near real-time system and must process up to 10,000 events per second (100 microseconds per event), iteration is not a feasible approach. The LDAR algorithm, while it has some flaws, is very rapid and efficient in reaching a solution. Analyses specific to the LDAR geometry and algorithm can be found in references 16, 17, 18, and 19. Another lightning detection system developed jointly between the University of Florida and KSC is called "TOA" and uses a very similar system geometry and the same location algorithm as described in LDAR [20].

The lightning time-of-arrival systems are generally grouped according to baseline length. Long baseline systems have receivers separated by kilometers or more and use recorded data to be correlated later or, in the case of LDAR, use microwave links to merge the data streams in real time. Short baseline systems are small enough so signals are carried to a

central point by cable. Long baseline systems can provide coverage in three dimensions to a large area, whereas short baseline systems are basically direction finders.

The background of radio direction finding of lightning events is nicely summarized by Uman [21, pg. 358]:

> "Oetzel and Pierce (1969) first suggested that a short baseline time-of-arrival technique could be used for locating lightning VHF sources. A criticism of short baseline systems and a discussion of the advantages and disadvantages of long and short baseline systems are given by Proctor (1973)...Basically with a short baseline system, pulse identification is no problem since the same pulse arrives at each of the closely spaced receivers in a time that is short compared to the time between pulses, and thus the sequences of pulses arrive at each receiver in the same order. On the other hand, a short baseline system produces at best a two dimensional direction: with two receivers one can obtain azimuth; with three receivers one can obtain both azimuth and elevation...Long baseline VHF time-of-arrival systems have the advantage of providing three-dimensional locations, but suffer the disadvantage of the difficulty in identifying VHF pulses from two or more simultaneous separated sources because the pulses arrive in a different order at each receiver."

For the reasons cited earlier in this document, the various combinations of receivers used by LDAR to form solutions often widely disagree. In addition, the multiple roots problem can result in a 180-degree directional error. The detailed reasons for this directional error in the algorithm are not known and, at present, cannot be internally detected using just the LDAR data. Tests conducted during this development project showed that roughly 60 percent of all events detected by LDAR are rejected based on bad comparisons between solutions provided by the 20 different subarrays of the system. An unknown percentage that is incorrect is passed forward as valid.

Direction-finding systems involving uncontrolled, nonperiodic pulse detection were found to be in a poor state of development. Some early work by Pierce and Oertzel was found to be along similar lines but much simpler than the approach taken here. No related work was found in the literature for the general problem encountered with the SBLDAR system, so one was developed. The approach to developing the SBLDAR algorithm was based on a noniterative approach in order to meet high processing speed requirements.

2. ALGORITHM DERIVATIONS

2.1 EQUATION FOR A SINGLE BASELINE

Any two receivers form a "baseline," that is a line connecting the two receiver coordinates. The location of a source S that produces a DTOA signal lies on a hyperbola

in the plane formed by the two antennas and the source (figure 1). Remember, that for each point on a hyperbola, the difference between the distances to the two foci is a constant. In this case, each antenna forms a focus of the hyperbola. This distance difference is the DTOA, in time units, times the speed of light c. Since the location of S and, hence, the orientation of the plane is unknown, one can only say that S lies on a "hyperbola of revolution" (i.e., a hyperbolic cone given by rotating the hyperbola around the axis defined by the baseline).

As the curve of a hyperbola is examined, further away from the origin, it asymptotically approaches a straight line that deviates from the baseline with interior angle ψ (figure 2). In SBLDAR, the only concern is with distant points relative to the length of the baselines. Therefore, the equations can be simplified by using only straight lines instead of hyperbolic curves. The error due to the assumption of the infinite source range R will be quantified later in the report. When the straight line is rotated about the axis, it generates a circular cone (figure 3).

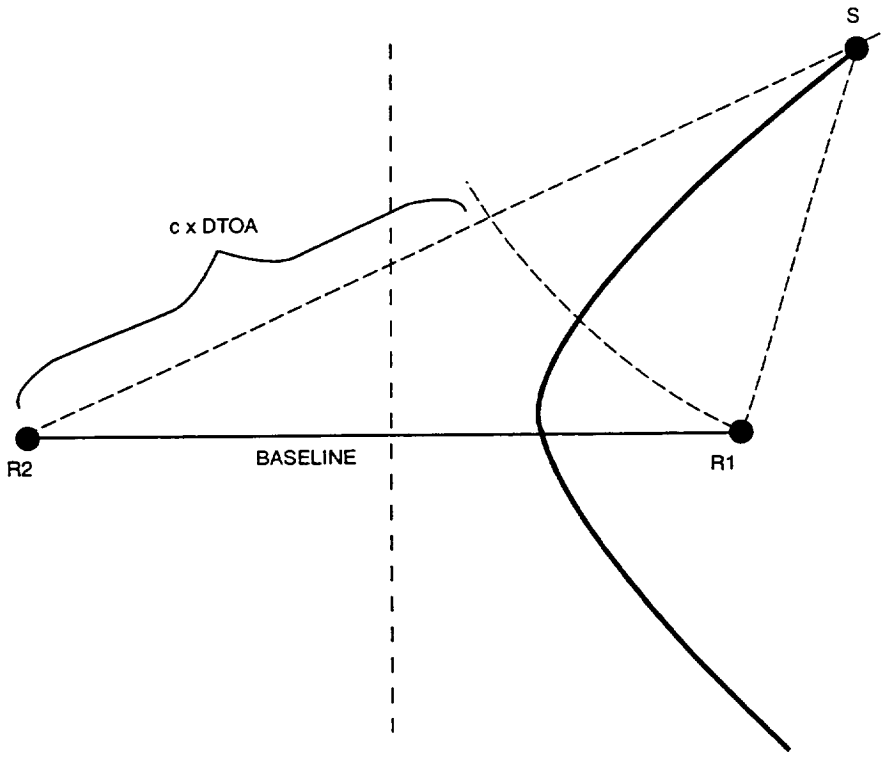

Figure 1. Location of a Source S Lies on a Hyperbola in the Plane Defined by S, R1, R2

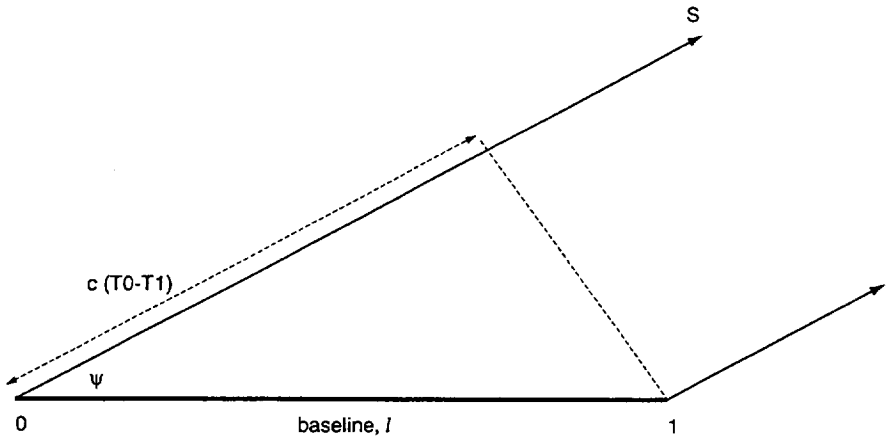

Figure 2. As "S" Goes to Infinity, cΔT Becomes Equal to lcosψ

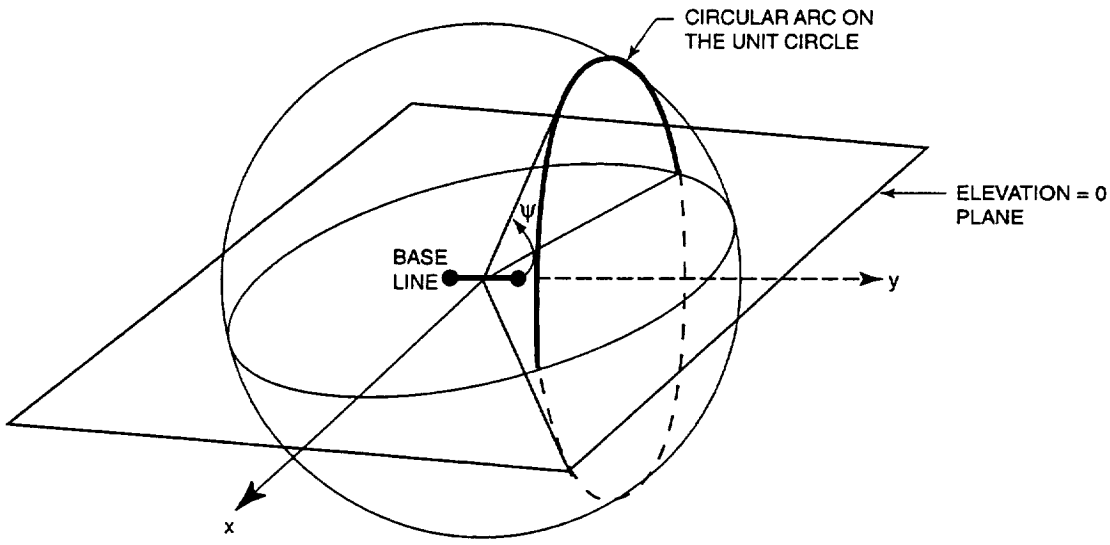

Figure 3. Cone Forms a Constant Angle ψ Between the Baseline and the Cone Surface

The SBLDAR system measures a time difference in nanoseconds between the time of signal arrival at one antenna minus the time of arrival to a second antenna. This DTOA times c, the speed of light, is a distance difference. If the measured TOA from antenna 1 as T1 is designated, it defines:

$$\Delta T_{01} = T0 - T1 \qquad (1)$$

If the ΔT_{01} term is positive, then T0 is a larger number and is later in time; the event reached "1" first. Therefore, the cone angles toward antenna 1. Likewise, if ΔT_{01} is negative, the event reached "0" first and the cone opening lies toward antenna 0 ($\psi > \pi/2$). The cone of constant ΔT_{01} forms a constant angle between the baseline and the cone surface ψ (figure 2). In terms of the ΔT_{01}, it can be seen that, for sources far away from the baseline:

$$c\Delta T_{01} = l_{01} \cos\psi \tag{2}$$

where l_{01} is the length of the baseline between receivers 1 and 0.

So that the cone angle ψ is given by:

$$\psi = \arccos\left(\frac{c}{l_{01}}(T0 - T1)\right) \tag{3}$$

This cone traces a circular arc on the sky. Using multiple baselines, multiple arcs can be produced such that their intersection defines the azimuth and elevation of the source. In order to accomplish this, the baseline orientation must be defined in terms of azimuth and elevation, which, coupled with the above DTOA equation, will allow the definition of the arc. Note also that for sources at infinite range, it can be assumed that the cone angle originates at the reference receiver and not at the midpoint between the two receivers.

2.2 DEFINITIONS OF COORDINATES

In this section, the AZ and EL angles are defined in terms of the local Cartesian coordinate system. It is necessary to express the orientation of each receiver pair baseline and the direction to each source in terms of AZ and EL. The locally flat Cartesian coordinate system is called (east, north, up) for (x, y, z), respectively. The AZ and EL angles are defined on figure 4. It is assumed that the reference receiver (point 0 in the SBLDAR system) lies at the point (x0, y0, z0) = (0, 0, 0).

The baseline vector is defined as the vector from (0, 0, 0) to the receiver listed first in the DTOA equation. For example, the baseline "10" vector runs from the point (0, 0, 0) to (x1, y1, z1). This vector defines a baseline orientation in terms of azimuth and elevation. The azimuth is measured from the north (y axis) in a clockwise direction. The elevation angle is measured up from the (x, y) plane. Points lying in the (x, y) plane define position vectors with a zero elevation angle.

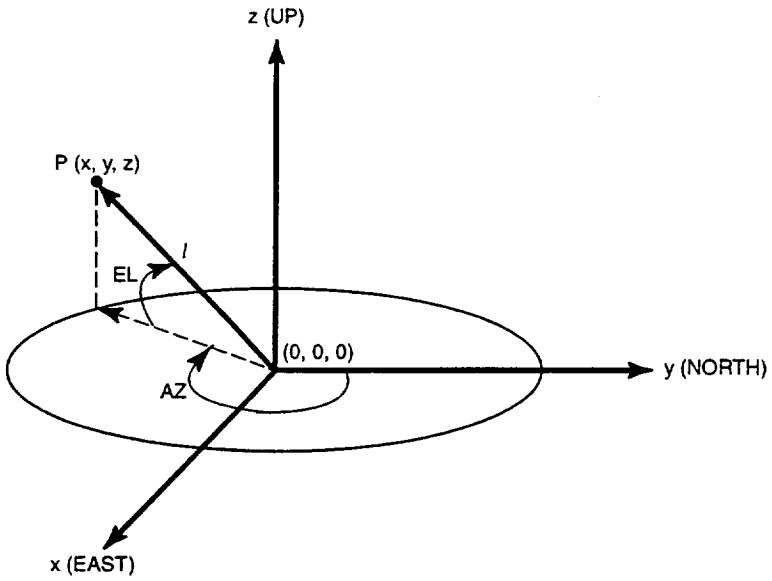

Figure 4. Definitions of Azimuth (AZ) and the Elevation Angle (EL)

The baseline vector is therefore given by:

$$\bar{l}_{10} = (x_1 - 0)\hat{i} + (y_1 - 0)\hat{j} + (z_1 - 0)\hat{k} \tag{4}$$

where $\hat{i}, \hat{j}, \hat{k}$ denote unit vectors along the x, y, and z axis, respectively.

The length of this vector is given by:

$$\left\|\bar{l}_{10}\right\| = \sqrt{x_1^2 + y_1^2 + z_1^2} = l_{10} \tag{5}$$

l_{10}, l_{20}, and l_{30} will be used to indicate the length of the three SBLDAR baselines vectors. It must be kept in mind that the results below will depend on the sign of the DTOA, which is implicitly affected by the direction assumed for the baseline vector.

To transform these results into AZ, EL, the transformations between spherical and Cartesian coordinates are recalled. Given a point $P(x_1, y_1, z_1)$, which could be an antenna or a source point, it can be transformed to spherical coordinates as follows, where again l_{10} is used to denote the length of the vector from the origin to the point (figure 4):

$$\begin{aligned} z_1 &= l_{10}\,\text{sinEL} \\ x_1 &= l_{10}\,\text{cosEL sinAZ} \\ y_1 &= l_{10}\,\text{cosEL cosAZ} \end{aligned} \tag{6}$$

Since the only interest is in AZ and EL, it is divided through by the length and solved for the angles:

$$EL = \arcsin\left(\frac{z_1}{l_{10}}\right) \tag{7a}$$

$$AZ = \arctan\left(\frac{x_1}{y_1}\right) \tag{7b}$$

Next, the angles of the baseline vector are defined using receiver 0 as the reference origin (0, 0, 0):

$$\begin{aligned} EL_{10} &= \arcsin\left(\frac{z_1}{\sqrt{x_1^2 + y_1^2 + z_1^2}}\right) \\ AZ_{10} &= \arctan\left(\frac{x_1}{y_1}\right) \end{aligned} \tag{8}$$

Equation 8 defines the AZ and EL of any point $P(x_1,y_1,z_1)$ in terms of the Cartesian system.

2.3 EQUATION FOR SINGLE BASELINE ARBITRARY ORIENTATION

This section derives the equation for the arc on the sky based on the measured delta T, baseline length, and baseline orientation. The following is a general treatment that can be solved for any baseline orientation. Given a source point $S(x_s, y_s, z_s)$ or, in spherical coordinates, S (l_s, AZ_s, El_s), and a baseline unit vector the following equation is applicable:

$$\hat{l}_{10} = \frac{x_1}{r_1}\hat{i} + \frac{y_1}{r_1}\hat{j} + \frac{z_1}{r_1}\hat{k} \tag{9}$$

Equations 10 and 11 express the vector pointing from the origin to the source point:

$$\vec{s} = x_s\hat{i} + y_s\hat{j} + z_s\hat{k} \tag{10}$$

and its corresponding unit vector:

$$\hat{s} = \frac{x_s}{r_s}\hat{i} + \frac{y_s}{r_s}\hat{j} + \frac{z_s}{r_s}\hat{k} \tag{11}$$

Note that the dot product between these two unit vectors is equal to the cosine of the angle between them.

$$\hat{s} \cdot \hat{l} = \cos\psi \tag{12}$$

The dot product is given by the sum of the products of the three components:

$$\hat{s} \cdot \hat{l} = \frac{x_S}{r_S} \cdot \frac{x_1}{r_1} + \frac{y_S}{r_S} \cdot \frac{y_1}{r_1} + \frac{z_S}{r_S} \cdot \frac{z_1}{r_1} \tag{13}$$

Equation 14 uses the following spherical coordinate conversion formulas (equation 6) to express the dot product in terms of angles:

$$\hat{s} \cdot \hat{l} = \cos EL_S \sin AZ_S \cos EL_1 \sin AZ_1 + \cos EL_S \cos AZ_S \cos EL_1 \cos AZ_1 + \sin EL_S \sin EL_1 \tag{14}$$

By rearranging, equation 15 is obtained:

$$\hat{s} \cdot \hat{l} = \cos EL_S \cos EL_1 \sin AZ_S \sin AZ_1 + \cos EL_S \cos EL_1 \cos AZ_S \cos AZ_1 + \sin EL_S \sin EL_1 \tag{15}$$

Using equation 2 to eliminate ψ, the DTOA equation for an arbitrary baseline becomes

$$\frac{c}{l_{01}}(T0 - T1) = \cos EL_S \cos EL_1 \sin AZ_S \sin AZ_1 + \cos EL_S \cos EL_1 \cos AZ_S \cos AZ_1 + \sin EL_S \sin EL_1 \tag{16}$$

One equation is provided by each baseline in the system. Two baselines are required to find a solution for AZ and EL. Three baselines provide an over determination of these variables, which allows the use of statistical techniques to reduce the measurement error. The system of three equations provided by a three-baseline array are typically not linear in AZ and EL and, therefore, tend to be difficult to solve. The goal is an array geometry that provides for accurate estimates of AZ and EL and is relatively easy to solve. A flat "Y" shaped array meets this requirement as is shown in the next section.

2.4 SBLDAR ALGORITHM

SBLDAR contains four antennas arrayed in a flat Y pattern with one in the center and three on symmetrical 300-foot (90-meter) nominal baselines at azimuths of $\pi/3$, π, and

$5\pi/3$ (AZ=0 north, measured from north to east, etc.). Cross-correlations are performed between the reference channel and each outer channel, in turn producing three data records of delta T's to provide azimuth and elevation estimates of the source location. The detector channels are numbered as follows:

0 = central (reference channel)
1 = northeast
2 = northwest
3 = south

The following equations are developed for each DTOA produced by a single source event (using equation 16 and noting that $\cos EL_{oi} = 1$ and $\sin EL_{oi} = 0$ for baselines in the ground plane):

$$\frac{c(T_0 - T_1)}{l_{01}} = (\cos EL_s)\ (\cos AZ_s \cos AZ_{01} + \sin AZ_s\ \sin AZ_{01})$$

$$\frac{c(T_0 - T_2)}{l_{02}} = (\cos EL_s)\ (\cos AZ_s \cos AZ_{02} + \sin AZ_s\ \sin AZ_{02}) \qquad (17)$$

$$\frac{c(T_0 - T_3)}{l_{03}} = (\cos EL_s)\ (\cos AZ_s \cos AZ_{03} + \sin AZ_s\ \sin AZ_{03})$$

These three equations can be cast as a set of linear equations by naming two unknowns, A and B.

$$A = \cos EL_S \cos AZ_S$$

$$B = \cos EL_S \sin AZ_S \qquad (18)$$

which results (in matrix form) in the following equation:

$$\begin{pmatrix} \frac{c}{l_{01}}(T_0 - T_1) \\ \frac{c}{l_{02}}(T_0 - T_2) \\ \frac{c}{l_{03}}(T_0 - T_3) \end{pmatrix} = \begin{pmatrix} \cos AZ_{01} & \sin AZ_{01} \\ \cos AZ_{02} & \sin AZ_{02} \\ \cos AZ_{03} & \sin AZ_{03} \end{pmatrix} \begin{pmatrix} A \\ B \end{pmatrix} \qquad (19)$$

Using the generalized inverse to solve for the matrix of unknowns A and B (inverse of H, when H is nonsquare is $(H^T H)^{-1} H^T$), the following equations are obtained:

$$A = \frac{(\Sigma \sin^2 AZ_{0i})(\Sigma \frac{c}{l} \cos AZ_{0i} \Delta T_{0i}) - (\Sigma \cos AZ_{0i} \sin AZ_{0i})(\Sigma \frac{c}{l} \sin AZ_{0i} \Delta T_{0i})}{\Sigma \sin^2 AZ_{0i} \Sigma \cos^2 AZ_{0i} - (\Sigma \cos AZ_{0i} \sin AZ_{0i})^2}$$

$$B = \frac{(\Sigma \cos AZ_{0i} \sin AZ_{0i})(\Sigma \frac{c}{l} \cos AZ_{0i} \Delta T_{0i}) - (\Sigma \cos^2 AZ_{0i})(\Sigma \frac{c}{l} \sin AZ_{0i} \Delta T_{0i})}{\Sigma \sin^2 AZ_{0i} \Sigma \cos^2 AZ_{0i} - (\Sigma \cos AZ_{0i} \sin AZ_{0i})^2} \quad (20)$$

The AZ_S and EL_S are solved for as follows:

$$EL_S = \cos^{-1}(\sqrt{A^2 + B^2}) \quad (21a)$$

$$AZ_S = \tan^{-1}\left(\frac{B}{A}\right) + n\pi \quad (n = 0, \pi \text{ or } 2\pi) \quad (21b)$$

where n is determined from the sign of A and B:

if SGN (A) = (+) and SGN (B) = (-); then n = 0

if SGN (A) = (-) and SGN (B) = (-); then n = 1

if SGN (A) = (-) and SGN (B) = (+); then n = 1

if SGN (A) = (+) and SGN (B) = (+); then n = 2 (22)

The sign evaluations are required due to the multiple values of the arctangent over the interval from 0 to 2π. Note that EL_S only ranges from 0 to $\pi/2$, so no ambiguity exists for the arc-cosine.

These coordinates are assumed to be in a local Cartesian frame centered on the center, or number 0, antenna. Making the following substitutions:

$$\sin AZ_{0i} = \frac{x_i}{l_i}$$

$$\cos AZ_{0i} = \frac{y_i}{l_i} \quad (23)$$

One then has equation 24:

$$A = \frac{\Sigma\left(\frac{x_{0i}^2}{l_{0i}^2}\right)\Sigma\left(\frac{c}{l_{0i}^2}\, y_{0i}\, \Delta T_{0i}\right) - \Sigma\left(\frac{y_{0i}\, x_{0i}}{l_{0i}^2}\right)\Sigma\left(\frac{c}{l_{0i}^2} x_{0i}\, \Delta T_{0i}\right)}{\left(\Sigma\frac{x_{0i}^2}{l_{0i}^2}\right)\left(\Sigma\frac{y_{0i}^2}{l_{0i}^2}\right) - \left(\Sigma\frac{x_{0i}\, y_{0i}}{l_{0i}^2}\right)^2}$$

$$B = \frac{\left(\Sigma\frac{x_{0i}\, y_{0i}}{l_{0i}^2}\right)\left(\Sigma\frac{c}{l_{0i}^2}\, y_{0i}\, \Delta T_{0i}\right) - \left(\Sigma\frac{y_{0i}^2}{l_{0i}^2}\right)\Sigma\left(\frac{c}{l_{0i}^2} x_{0i}\, \Delta T_{0i}\right)}{\Sigma\left(\frac{x_{0i}^2}{l_{0i}^2}\right)\Sigma\left(\frac{y_{0i}^2}{l_{0i}^2}\right) - \left(\Sigma\frac{y_{0i}\, x_{0i}}{l_{0i}}\right)^2} \qquad (24)$$

These exact formulas are used for the analysis of data from the SBLDAR system. This last formula also simplifies the use of this approach for nonsymmetrical arrays.

An approximate form of the above equations for A and B can be formed using the three baseline azimuths of $\pi/3$, π, and $5\pi/3$, and assuming equal baseline lengths as follows:

$$A = \left(\frac{c}{l \cdot 1.5}\right)\left(\frac{1}{2}\right)\left(\Delta T_{01} + \Delta T_{02} - 2\Delta T_{03}\right) \qquad (25)$$

$$B = \left(\frac{c}{l \cdot 1.5}\right)\left(\sqrt{\frac{3}{4}}\right)\left(\Delta T_{01} - \Delta T_{02}\right) \qquad (26)$$

The above formulas are not exact because the SBLDAR array is not perfectly symmetrical but are extremely close for the array built. This form of the equations will facilitate the error analyses that follow.

3. ERROR ANALYSES

3.1 SOURCES OF ERRORS IN AZ AND EL ESTIMATES

Each measurement provides an arc that makes a large circle on the sky (see figure 3). If the measurements contain some errors, the three circles will not intersect at a single point but will form a triangle as shown in figure 5. Each corner of the triangle represents the

AZ and EL solution found using only two of the three baselines. The question is where in AZ and EL is the "best" or most probable solution given the measured ΔT's?

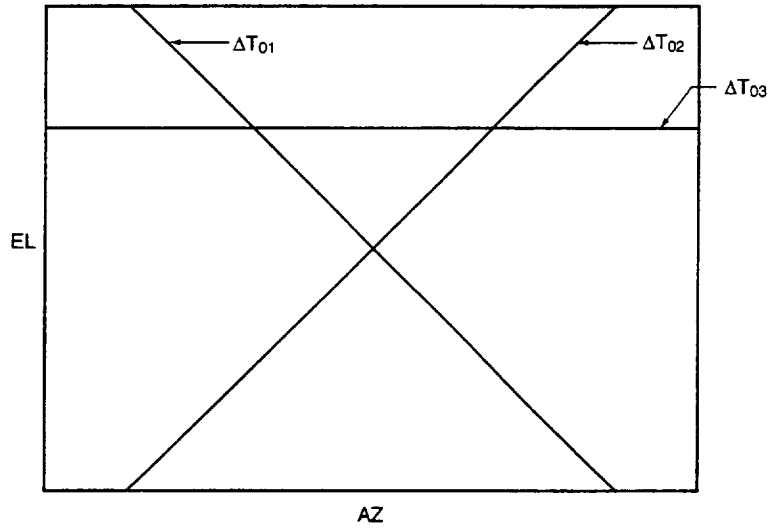

Figure 5. Close-Up View of the Intersection of the Three Lines of Position

The algorithm contained in this document provides a minimum squared error solution to the positioning problem such that the estimate of AZ and EL is in the middle of the triangle formed by the lines of position in figure 5. This may not be the optimal solution due to the high magnification of random errors by measurements that occur nearly along a given baseline. Future algorithms may incorporate a weighted least squares approach that weights the contribution from each baseline based on its inherent magnification of errors.

Measurement errors consist of random and bias errors. Random errors are due to noise and other random processes in the measurement chain. Random errors are typically minimized by averaging a number of measurements. This is not possible in a lightning measurement system since the event only occurs once. Bias errors can, at least in theory, be eliminated through a process of calibration and affect, in some consistent way, all measurements. Bias errors that are unknown are generally treated as random because they are unknown.

Sources of error in the SBLDAR system include:

a. Determination of DTOA's:

(1) Measurement noise resulting in poor matching of each antenna's time history signal (random)

(2) Digitizing error (random)

(3) Aliasing of unfiltered high frequency signal components to lower frequencies (random)

(4) Time jitter in the analog-to-digital conversion stage (random)

(5) Multipath errors (again causing differences between channels)(random)

(6) Error in the polynomial curve fit of the correlation function (random)

(7) Errors in the relative channel time delays (delta K's) due to cable lengths, filters, and other differences (systematic or bias error)

(8) Movement in the source during the RF emission process or other effects that result in the lightning source not being a point source (random)

(9) Errors caused by changes in ambient temperature affecting cables and electronics (bias)

(10) Errors caused by changes in the atmospheric index of refraction gradient (bias)

b. Computation of AZ and EL:

(1) Poor baseline geometry resulting in amplification of errors (random for any particular direction of source, depends on source AZ and EL and on the baseline geometry)

(2) Numerical error growth in algorithm due to singularities in the math or nearly singular matrices (typically random)

(3) Errors due to finite source range (which is assumed to be infinite in the algorithm)(systematic)

(4) Errors due to mixing of accurate and inaccurate baseline data (use of a DTOA measured nearly along the baseline and at a high random error) (random)

(5) Offsets between the SBLDAR from the LDAR reference antenna (systematic)

This document only addresses the errors in computing the AZ and EL values from the set of provided DTOA's. This report examines ways to mitigate the sources of the errors listed in 3.1.b to maximize the accuracy and precision of the SBLDAR design.

To find how each measurement may be affected by random errors, using equation 2 the derivatives of both sides are taken.

$$cd\Delta T = -l\sin\psi\, d\psi \tag{27}$$

By rearranging equation 27, equation 28 is obtained:

$$\frac{d\psi}{d\Delta T} = \left(\frac{c}{l}\right)\frac{-1}{\sin\psi} \tag{28}$$

This expression can be interpreted as the ratio of standard deviations. Taking the absolute value (since the timing error can be positive or negative), equation 29 is obtained.

$$\sigma_\psi = \left(\frac{c}{l}\right)\frac{1}{\sin\psi}\sigma_{\Delta T} \tag{29}$$

If the standard deviation of the timing difference error is 1 nanosecond (ns), the baseline length is 90 meters; and, using a value of c equal to 0.2997 m/ns, it is evident that equation 30 applies.

$$\sigma_\psi = \frac{0.0033}{\sin\psi}\times\left(\frac{180}{\pi}\right)[\text{degrees/ns}] \tag{30}$$

The last term is to convert from radians to degrees. The best accuracy is achieved when the source is at right angles to the baseline and, for SBLDAR, is equal to 0.19 degrees per nanosecond timing accuracy (in the absence of other errors). Figure 6 shows the angular accuracy as a function of ψ ("delta psi" denotes σ_ψ the standard deviation of ψ as given in equation 30):

This means that, in areas where a given baseline is parallel or nearly parallel to the incoming rays, it should probably be excluded from the solution; however, the current algorithm does not exclude any baselines.

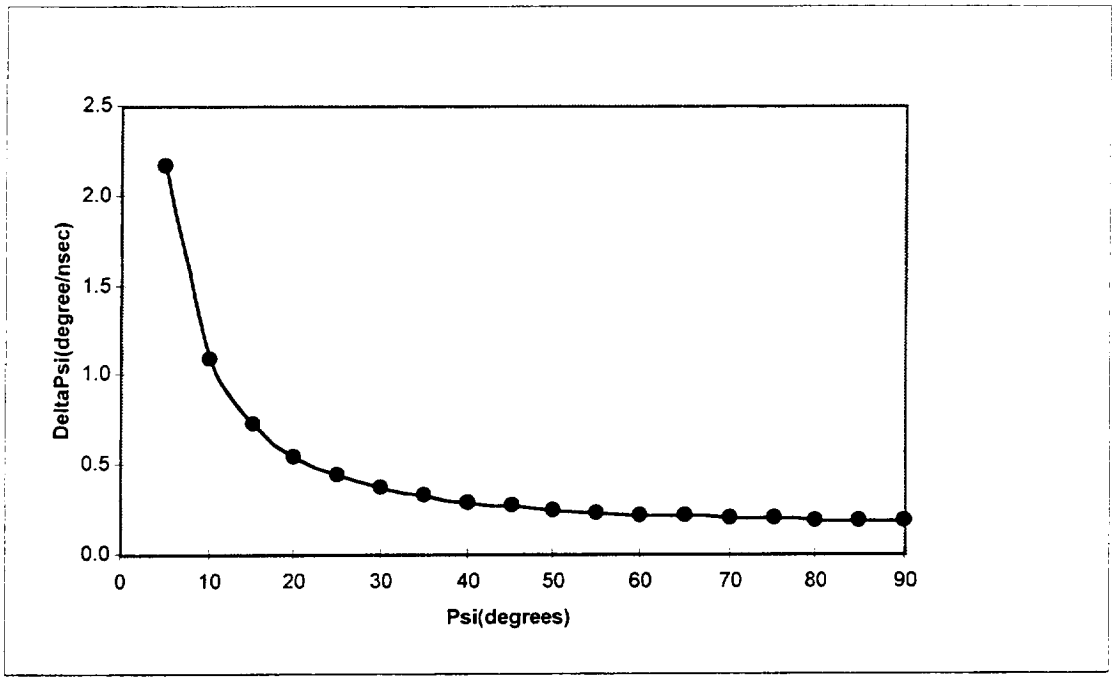

Figure 6. Angle Measurement Error as a Function of the Angle Formed Between the Baseline and the Source Vector for 90-Meter Baseline and 1-Nanosecond Timing Error

The next sections examine how these baseline random errors are combined through the SBLDAR algorithm to result in errors in AZ and EL. The method chosen is that of dilution of precision (DOP), which is equal to the ratio of the root mean square (rms) angular error (in AZ or EL) divided by the rms error in the delta T measurements. Surprisingly, the azimuth dilution of precision (AZDOP) and elevation dilution of precision (ELDOP) formulas do not directly use the results of the previous section.

3.2 DERIVATION OF AZDOP

The process starts with the equations for the azimuth of the source (same as equation 21b).

$$\mathrm{AZ}_S = \tan^{-1}\left(\frac{B}{A}\right) + n\pi \quad (n = 0, \pi \text{ or } 2\pi) \tag{31}$$

where (same as 25 and 26) the following applies:

$$\mathrm{A} = \left(\frac{c}{l \cdot 1.5}\right)\left(\frac{1}{2}\right)\left(\Delta T_{01} + \Delta T_{02} - 2\Delta T_{03}\right) \tag{32a}$$

$$B = \left(\frac{c}{l \cdot 1.5}\right)\left(\sqrt{\frac{3}{4}}\right)\left(\Delta T_{01} - \Delta T_{02}\right) \tag{32b}$$

Calculus can be used to determine the effect of errors in the delta T's in solving for the AZ. Because there is a functional relationship between the measured variables (the delta T's) and the estimated variable AZ, one can take the total derivative of the AZ with respect to each delta T according to the following formula from calculus:

$$dAZ_S = \left(\frac{\partial AZ_S}{\partial \Delta T_{01}}\right) d\Delta T_{01} + \left(\frac{\partial AZ_S}{\partial \Delta T_{02}}\right) d\Delta T_{02} + \left(\frac{\partial AZ_S}{\partial \Delta T_{03}}\right) d\Delta T_{03} \tag{33}$$

The dAZ_S term is taken to represent the total error in the estimated variable and the $d\Delta T$ terms to represent the errors in the measured variables. The point of interest is the root mean squared error because the specific errors could be positive or negative; so the square of both sides and the square root is taken to get equation 34.

$$\left(dAZ_S\right)_{rms} = \sqrt{\left(\frac{\partial AZ_S}{\partial \Delta T_{01}}\right)^2 d\Delta T_{01}^2 + \left(\frac{\partial AZ_S}{\partial \Delta T_{02}}\right)^2 d\Delta T_{02}^2 + \left(\frac{\partial AZ_S}{\partial \Delta T_{03}}\right)^2 d\Delta T_{03}^2} \tag{34}$$

Note that it was assumed that the delta T's are uncorrelated, at least to the extent that the cross terms are insignificantly small. Next, the definition of AZDOP is used and the standard assumption in its derivation is made that the expected errors in the delta T's are equal to one. This is one in whatever units desired, but it is assumed 1 nanosecond errors. The definition of AZDOP lets one use whatever units desired as long as the errors are small enough that the implicit assumptions remain correct. The result is then scaled to the actual timing errors. This assumption allows the removal of the delta T terms from the radical as follows:

$$AZDOP \equiv \frac{\left(dAZ_S\right)_{rms}}{\left(d\Delta T\right)_{rms}} = \sqrt{\left(\frac{\partial AZ_S}{\partial \Delta T_{01}}\right)^2 + \left(\frac{\partial AZ_S}{\partial \Delta T_{02}}\right)^2 + \left(\frac{\partial AZ_S}{\partial \Delta T_{03}}\right)^2} \tag{35}$$

This formula enables the error in azimuth to be estimated if the basic measurement error in nanoseconds is known or can be estimated. The next step is to analytically produce the three terms under the radical given one's knowledge of the equations. Since the derivative of the arctangent will be taken, the formula in the Chemical Rubber Company (CRC) Standard Mathematical Tables, 21st Edition, page 404 [22] is used:

$$\frac{d}{dx}(\arctan u) = \frac{1}{1+u^2}\frac{du}{dx}, \quad \left(-\frac{\pi}{2} < \arctan u < \frac{\pi}{2}\right) \tag{36}$$

This derivative is evaluated as three terms, one for each term under the radical of the AZDOP equation. All three terms have the 1 over 1 plus u squared term in common, so it is evaluated first (leaving it in terms of A and B).

$$\frac{1}{1+u^2}=\frac{1}{1+\left(\frac{B}{A}\right)^2}=\frac{A^2}{A^2+B^2} \tag{37}$$

This term will be squared in each of the three terms, summed out, then square rooted back to its original form in the AZDOP equation. Next, the first of the three derivative terms is evaluated.

$$\frac{\partial AZ_S}{\partial \Delta T_{01}}=\sqrt{\frac{3/4}{1/4}}\frac{\partial}{\partial \Delta T_{01}}\left\{\frac{\Delta T_{01}-\Delta T_{02}}{\Delta T_{01}+\Delta T_{02}-2\Delta T_{03}}\right\} \tag{38}$$

Working through the derivatives and converting to an expression in terms of A and B results in equation 39.

$$\frac{\partial AZ_S}{\partial \Delta T_{01}}=\frac{c}{l\cdot 1.5}\left\{\frac{\sqrt{3/4}\,A+1/2\,B}{A^2}\right\} \tag{39}$$

Likewise, the next term is evaluated as the following:

$$\frac{\partial AZ_S}{\partial \Delta T_{02}}=-\frac{c}{l\cdot 1.5}\left\{\frac{\sqrt{3/4}\,A-1/2\,B}{A^2}\right\} \tag{40}$$

and the last term is equation 41:

$$\frac{\partial AZ_S}{\partial \Delta T_{03}}=-\frac{c}{l\cdot 1.5}\left\{\frac{B}{A^2}\right\} \tag{41}$$

By combining these terms together, equation 42 is obtained.

$$AZDOP=\left(\frac{c}{l\cdot 1.5}\right)\left(\frac{A^2}{A^2+B^2}\right)\sqrt{\left(\frac{\sqrt{3/4}\,A+1/2\,B}{A^2}\right)^2+\left(\frac{-\sqrt{3/4}\,A+1/2\,B}{A^2}\right)^2+\left(\frac{B}{A^2}\right)^2} \tag{42}$$

This simplifies to the following equation:

$$\text{AZDOP} = \frac{c}{l \cdot \sqrt{1.5}} \frac{1}{\sqrt{A^2 + B^2}} = \frac{c}{l \cdot \sqrt{1.5}} \frac{1}{\cos \text{EL}_S} \left(\frac{180}{\pi} \right) \tag{43}$$

The last term converts the result to degrees per nanosecond. We thus derive the result that the azimuth error, for our array geometry, does not depend on the azimuth angle itself.

3.3 DERIVATION OF ELDOP FOR THE Y ARRAY

A similar exercise is followed to derive the expression for ELDOP using the CRC formula [12] for the derivative of arc-cosine.

$$\frac{d}{dx}(\arccos u) = -\frac{1}{\sqrt{1-u^2}} \frac{du}{dx}, \quad (0 \leq \arccos u \leq \pi) \tag{44}$$

The ELDOP is defined as:

$$\text{ELDOP} \equiv \frac{(d\text{EL}_S)_{rms}}{(d\Delta T)_{rms}} = \sqrt{\left(\frac{\partial \text{EL}_S}{\partial \Delta T_{01}} \right)^2 + \left(\frac{\partial \text{EL}_S}{\partial \Delta T_{02}} \right)^2 + \left(\frac{\partial \text{EL}_S}{\partial \Delta T_{03}} \right)^2} \tag{45}$$

First, the one over square root term is evaluated.

$$-\frac{1}{\sqrt{1-u^2}} = \frac{-1}{\sqrt{1-\left(\sqrt{A^2+B^2}\right)^2}} = \frac{-1}{\sqrt{1-\cos^2 EL_S}} = \frac{-1}{\sin EL_S} \tag{46}$$

Next, by evaluating each of the three partial derivative terms as before, the equation in terms of the delta T's is recast.

$$\cos^{-1}\left(\sqrt{A^2+B^2}\right) = \cos^{-1}\left(\left(\frac{c}{l \cdot 1.5} \right) \sqrt{\Delta T_{01}^2 + \Delta T_{02}^2 + \Delta T_{03}^2 - \Delta T_{01}\Delta T_{02} - \Delta T_{01}\Delta T_{03} - \Delta T_{02}\Delta T_{03}} \right) \tag{47}$$

Proceeding as before, equation 48 is obtained.

$$\frac{\partial u}{\partial \Delta T_{12}} = \frac{(c/l \cdot 1.5)(2\Delta T_{01} - \Delta T_{02} - \Delta T_{03})}{\sqrt{\Delta T_{01}^2 + \Delta T_{02}^2 + \Delta T_{03}^2 - \Delta T_{01}\Delta T_{02} - \Delta T_{01}\Delta T_{03} - \Delta T_{02}\Delta T_{03}}} \tag{48}$$

The remaining two terms are likewise found to be the following:

$$\frac{\partial u}{\partial \Delta T_{32}} = \frac{(c/l \cdot 1.5)(2\Delta T_{02} - \Delta T_{01} - \Delta T_{03})}{\sqrt{\Delta T_{01}^2 + \Delta T_{02}^2 + \Delta T_{03}^2 - \Delta T_{01}\Delta T_{02} - \Delta T_{01}\Delta T_{03} - \Delta T_{02}\Delta T_{03}}} \tag{49}$$

$$\frac{\partial u}{\partial \Delta T_{42}} = \frac{(c/l \cdot 1.5)(2\Delta T_{03} - \Delta T_{01} - \Delta T_{02})}{\sqrt{\Delta T_{01}^2 + \Delta T_{02}^2 + \Delta T_{03}^2 - \Delta T_{01}\Delta T_{02} - \Delta T_{01}\Delta T_{03} - \Delta T_{02}\Delta T_{03}}} \tag{50}$$

Taking the root of the sum of squares of equations 48, 49, and 50 results in the lengthy term in the radical sign canceling (details left to the reader), and the resulting ELDOP expression is equation 51:

$$\text{ELDOP} = \frac{\sqrt{6}\ c}{l \cdot 1.5}\left(\frac{1}{\sin EL_S}\right)\left(\frac{180}{\pi}\right)[\text{degrees/ ns}] \tag{51}$$

Note that the equation for ELDOP and, therefore, the amplification of errors goes to infinity at zero elevation. This is a concern because most detected events will be distant from the array and will be at low elevation angle.

3.4 ELEVATION ANGLES AND ELDOP DERIVED FROM A VERTICAL BASELINE

The SBLDAR system also has a vertical baseline consisting of two antennae mounted on a tower, near the Y array, with a vertical separation of about 20 meters. This section addresses the use of this vertical baseline to improve the elevation angle accuracy of the SBLDAR system. Almost by inspection from equation 16, it can be seen that when the baseline is vertical and, therefore, has no azimuth components, the measurement equation becomes the following:

$$(T_B - T_T) = \frac{l}{c}\sin EL \tag{52}$$

T_B and T_T represent TOA's for the bottom antenna and top antenna respectively, and l is the height of the baseline. Solving for EL, the following expression is obtained:

$$EL = \sin^{-1}\left((T_B - T_T)\frac{c}{l}\right), \text{ where } 0 < EL < \pi/2. \tag{53}$$

An error analysis can immediately be performed to determine the propagation of timing errors into elevation angle errors. This is done by taking the Taylor series expansion of the sine of EL in terms of the delta T expression from the measured values to the actual value.

$$(\Delta T)_{act} - (\Delta T)_{meas} = \{(EL)_{meas} - (EL)_{act}\}\left(\frac{l}{c}\right)\cos EL \qquad (54)$$

If the formula is made more concise, the following expression is obtained:

$$\frac{dEL}{d\Delta T} = \left(\frac{c}{l}\right)\frac{1}{\cos EL} \qquad (55)$$

The error is a minimum when the elevation is zero and a maximum at the zenith. Note, however, that at higher elevation angles, the Taylor series in error would need to include some higher order terms. So this expression somewhat over estimates the error at high EL. ELDOP is defined by:

$$ELDOP = \frac{c}{l}\left(\frac{1}{\cos EL_S}\right)\left(\frac{180}{\pi}\right)[\text{degrees/ ns}] \qquad (56)$$

This suggests that there is significant benefit in providing for a vertical baseline when events are to be detected at low elevations. The expression also allows for the evaluation of needed vertical baseline height for a given error reduction. The cost of baseline height is very expensive in the case of an array of sensors such as the SBLDAR system. An evaluation of the benefits of a vertical array should include an analysis of the mask angle of the antenna design chosen and the effect of the terrain so that the lowest useful elevation angle for actually detecting events is considered. In figure 7 for example, for equal timing errors and a vertical baseline of 20 meters coupled to a Y array of 90 meters baseline, the two ELDOP curves cross at 20 degrees. Mask angles of 15 degrees are not uncommon, so the benefit of the vertical array may only be realized for events below 20 and above 15 degrees.

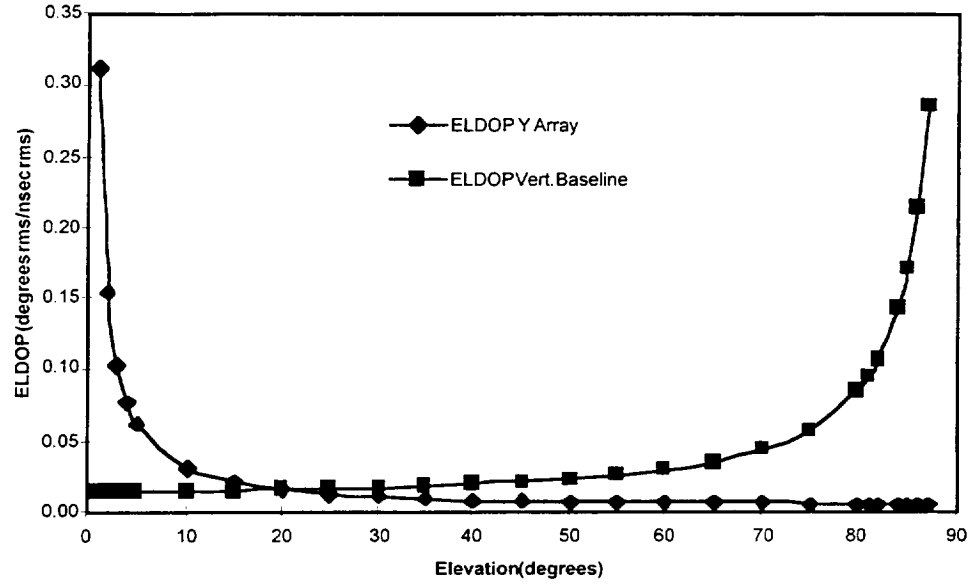

Figure 7. ELDOP for a Vertical Baseline of 20 Meters Versus the ELDOP for an SBLDAR 90-Meter Flat Array

3.5 EFFECT OF CURVATURE (FINITE SOURCE RANGE) ON THE MEASURED DTOA's

The preceding analyses assumed explicitly that the wave front was flat, meaning that the source was at an infinite distance R. If the source is at a finite distance, the time of arrival at the remote detector will be somewhat later than the arrival time from a source in the same direction at infinity (i.e., the delta T will be increased). This can be conceptualized for this array, where there are a series of detectors laid out on a circle surrounding the reference detector. If a snapshot is made of the phase front that passes through the circle formed by the array at the moment the phase front is at the central detector, a disc tilted with respect to the detector array circle is obtained. If the source is at infinity, the disc is flat. For a symmetric array (i.e., the angles between the baselines are equal), this results in the sum of delta T's between the central and remote detectors equaling zero. If the source is not at infinity, the disc is curved up at the edges so each delta T is increased by the addition of a positive component and the sum of delta T's is a positive number. This can perhaps be best visualized when the source is straight up and the phase front is shaped like a bowl.

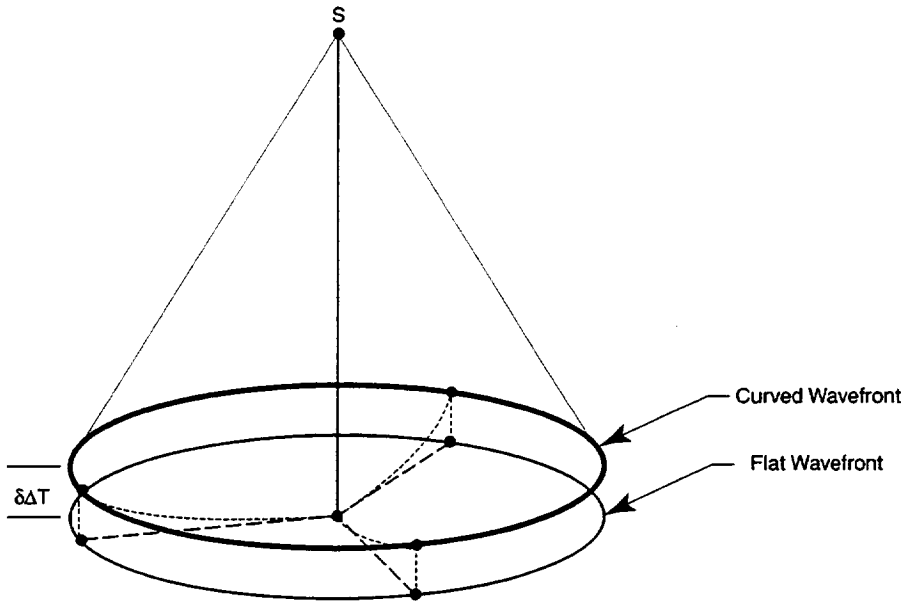

Figure 8. Source at Finite Distance Produces an Additional Delta T ($\delta\Delta T$) Due to Curvature of the Wavefront (Pictured is the wavefront from S, straight over the control receiver, showing the wavefront at the moment of contact with receiver zero.)

Figure 9 quantifies the error resulting from ignoring the wavefront curvature. The figure was produced by computing the angle ψ for points along an actual angle to the baseline as shown in the legend (15, 25, 35, 50, and 85 degrees). As expected, the error decreases as the range increases since equation 16 was derived assuming a source at infinity. It also shows that less error occurs at low angles. This chart can be used for choosing an appropriate baseline length or for determining, for given accuracy requirements, the need for correcting for wavefront curvature.

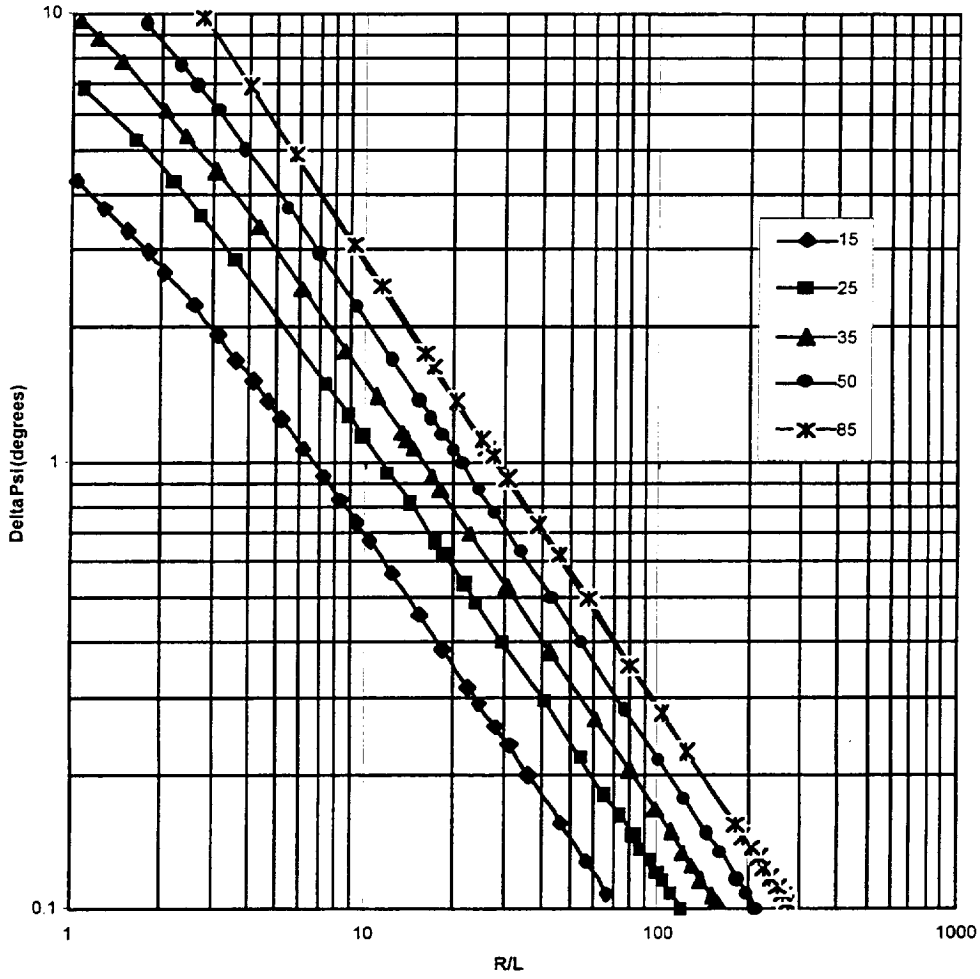

Figure 9. Error in Angle as a Function of Slant Range From a Single Baseline Using Equation 16 Without Accounting for Wavefront Curvature

To derive equations for the effect of wavefront curvature, or finite source range, note figure 10 which shows, for a source directly over the baseline, a triangle with an inscribed segment of a circle of radius R. The base of the triangle is twice the baseline l. The quantity Δr is the additional distance for the wave front (the curved segment) to travel before it reaches the remote detector compared to a flat phase front (the triangle's base). The length of one of the triangle's sides is given by $R + \Delta r$. Using the Pythagorean Theorem on the right triangle, equation 57 is obtained.

$$(\Delta r + R)^2 = l^2 + R^2 \tag{57}$$

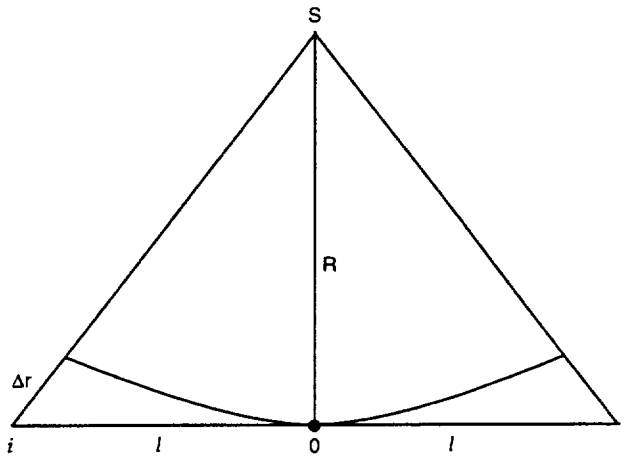

Figure 10. Solving for the Increased DTOA Due to the Curvature of the Wavefront With the Source Direction is at a Right Angle to the Baseline.

Rearranging to solve for Δr, equation 58 is obtained.

$$\Delta r \cong \frac{l^2}{2R} \tag{58}$$

It was assumed that $\Delta r << R$. Note an approximation can be provided to any level of accuracy by expanding a small ratio term (nearly 1) in a power series. For this case, R is generally greater than 10 times the size of Δr, so the approximation is adequate.

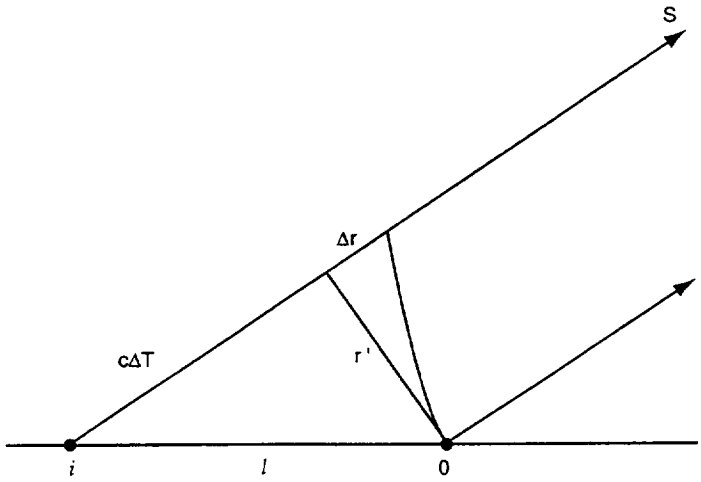

Figure 11. Solving for the Increased DTOA Due to the Curvature of the Wavefront With the Source Direction at a Lesser Angle to the Baseline (General Case)

This expression can be converted directly to additional DTOA when the source direction is at a right angle to the baseline as in figure 10. This DTOA is reduced as the baseline direction becomes closer to the source direction until no correction is required when the two are collinear. Therefore, an expression is needed for the perpendicular distance. Figure 11 shows the case for a source direction at a lesser angle to the baseline. It is first noted that, in the case of a plane wave, the baseline (time delay times c) and this perpendicular distance form a right triangle. The hypotenuse of the triangle is the baseline length l. Denoting the perpendicular distance as r', equation 59 is obtained:

$$l^2 = c^2\Delta T^2 + (r')^2 \tag{59}$$

By substituting into the above expression for Δr and replacing l with r', equation 60 is obtained.

$$\Delta r = \frac{l^2}{2R}\left(1 - \frac{c^2\Delta T^2}{l^2}\right) \tag{60}$$

Since the Δr term can be denoted as $\delta\Delta T$ as a correction to the plane wave ΔT, equation 61 is obtained.

$$\delta\Delta T = \frac{l^2}{2\,c\,R}\left(1 - \frac{c^2\Delta T^2}{l^2}\right) \tag{61}$$

As can be verified by performing the summation analytically, for a plane wave, the sum of the three baseline ΔT's is equal to zero (with no noise). Since each of the $\delta\Delta T$'s is positive, the sum of measured ΔT's should equal the sum of the $\delta\Delta T$'s. Therefore, the three equations for the $\delta\Delta T$'s can be summed and solved for R explicitly:

$$R = \left\{ \frac{\frac{l^2}{2\,c}\left(3 - \frac{c^2}{l^2}\sum_i \Delta T_{01}^2\right)}{\sum_i \Delta T_{01}} \right\} \tag{62}$$

The complete equation for each baseline ΔT can be expressed by combining equation 61 with equation 16 for the total delta T.

$$(T_0 - T_i) = \frac{l}{c}\left(\cos EL_S \cos\left(AZ_S - AZ_{0i}\right)\right) + \frac{l^2}{2cR}\left(1 - \cos^2 EL_s \cos^2\left(AZ_S - AZ_{0i}\right)\right) \quad (63)$$

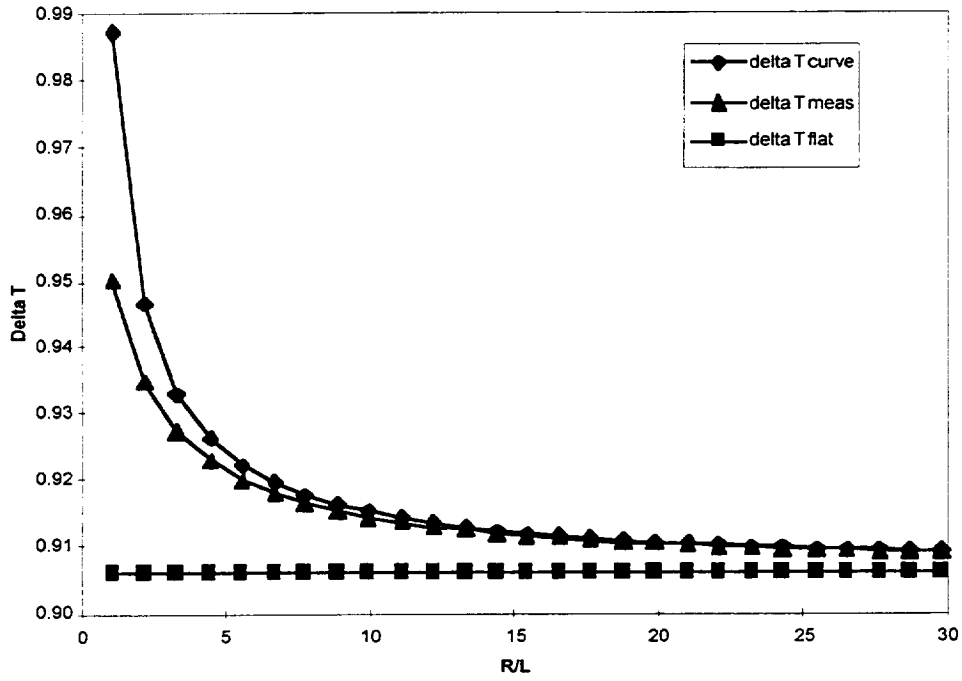

Figure 12. Delta T Predicted by Equation 63 "delta T curve" Compared to Equation 16 "delta T flat" and Actual Computed Delta T "delta T meas" Using Points Along a Constant 25-Degree Baseline Angle as the Slant Range is Varied

Note that finite range always increases the DTOA compared with that from an infinitely distant source. Also note, as shown in figure 12, that while equation 63 is much more accurate than equation 16, it overpredicts the DTOA at close range.

It is possible to solve for range using equation 62 then solve for a correction to the derived AZ and EL. Another method would be to use the AZ, EL derived from equation 16 and the range from equation 62 as a first step in an iteration solution (nonlinear least squares) for R, AZ, and EL.

3.6 SBLDAR FIXED DELAYS (K FACTORS)

The radiated impulse test consists of using an antenna at a surveyed location to radiate an impulse that is received by the SBLDAR antennae. The signals travel a known distance from the source location to each antenna then travel down the antenna cables, through filters, etc., until the data is digitized and recorded.

Differences between the channel time delays create a bias error or unchanging shift in the delta T's computed for each channel pair. If point "*r*" is designated as the known radiating location and "i" as the receiving antenna/channel, the time delay from the moment of radiation to the moment of data recording is given by equation 64:

$$T_i' - T_r = \frac{R_{ir}}{c} + K_i \tag{64}$$

K_i is the time delay between the antenna and time tagging for the i^{th} channel and T_i' is the raw received time. If K_i were zero, the time difference would only be due to propagation delays and the unprimed T_i could be used. The value R is the geometric distance between the radiating and receiving antennae. The symbol c is the speed of light. If data from two channels is cross correlated, equation 65 is obtained.

$$\Delta T_{ij}' = \left(T_i' - T_r\right) - \left(T_j' - T_r\right) = \frac{R_{ir} - R_{jr}}{c} + \left(K_i - K_j\right) \tag{65}$$

The unknowns in this equation are the K's, because the geometric ranges can be computed from the survey data. The resulting equation for each pair of channels is:

$$K_i - K_j = \Delta T_{ij}' + \frac{R_{ir} - R_{jr}}{c} \tag{66}$$

Each time delta T data is taken, it must be corrected by the delta K's in order to realize a true DTOA. Note also that the errors in determining the survey locations of the radiating point and each antenna become part of the total error budget, as bias error, in all AZ, EL solutions. The correct (unprimed) delta T's are given by equation 67:

$$\Delta T_{ij} = \Delta T_{ij}' - \left(K_j - K_i\right) \tag{67}$$

Accurate determination of the ΔK's may be very difficult and may be the largest source of error in establishing the position of lightning events.

3.7 SBLDAR ERRORS DUE TO OFFSET BETWEEN SBLDAR ORIGIN AND LDAR ORIGIN

The EL and AZ estimates are compared with LDAR data that has a different origin, the LDAR central-site antenna. The vector $\overline{D}$ is the vector pointing from the SBLDAR origin to the LDAR origin. AZ and EL are the angles measured from the SBLDAR system while AZ' and EL' are measured from the LDAR origin. The source of the lightning is at S. It is also assumed that there is no elevation difference between the LDAR and SBLDAR originals (Z = Z').

Conceptually, it can be seen that, if S is at infinity, the AZ and EL angles are equal between the two systems. The elevation difference ΔEL is a maximum if the source lies along the azimuth direction of $\underline{D}$. The ΔEL in this case can be derived using the following diagram (see figure 13).

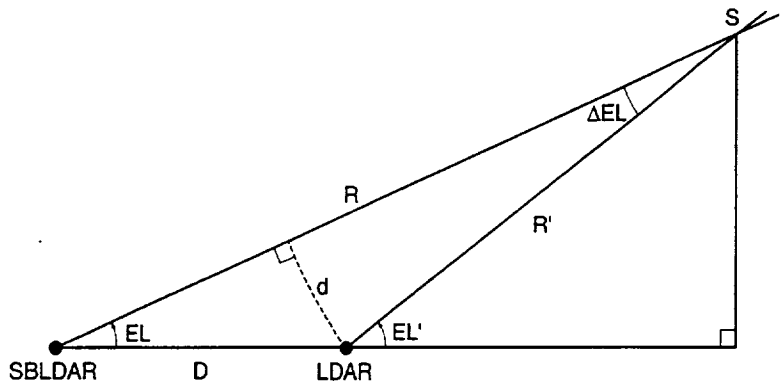

Figure 13. Geometry for SBLDAR EL Correction to LDAR Coordinates

By dropping a perpendicular from R to the LDAR origin called d,

$$R' \sin \Delta EL = d \tag{68}$$

and

$$D \sin EL = d \tag{69}$$

d is eliminated, and by simplifying and using the relationship for small angles

$$\sin \Delta EL \cong \Delta EL \tag{70}$$

equation 71 is obtained

$$\Delta EL = \frac{D}{R'} \sin EL \tag{71}$$

For small ΔEL, R' and R are nearly equal, equation 72 is obtained for sources along the direction $\overline{D}$.

$$EL' = EL + \frac{D}{R} \sin EL \tag{72}$$

Because at azimuths at right angles to $\underline{D}$ the elevation angles will be equal, it can be argued that the second term is modified by a cosine function in azimuth as measured from the direction of $\underline{D}$.

$$EL' = EL + \frac{D}{R} \sin EL \cos(AZ + AZ_D) \tag{73}$$

or in terms of the X and Y components of $\overline{D}$

$$EL' = EL + \frac{D}{R} (\sin EL)(\cos (AZ + \tan^{-1}\left(\frac{YD}{XD}\right)) \tag{74}$$

To solve for ΔAZ, note that ΔAZ will be zero for sources in the azimuth direction of $\overline{D}$ and a maximum along azimuths perpendicular to $\overline{D}$. Figure 14 is used to solve for ΔAZ (equation 75).

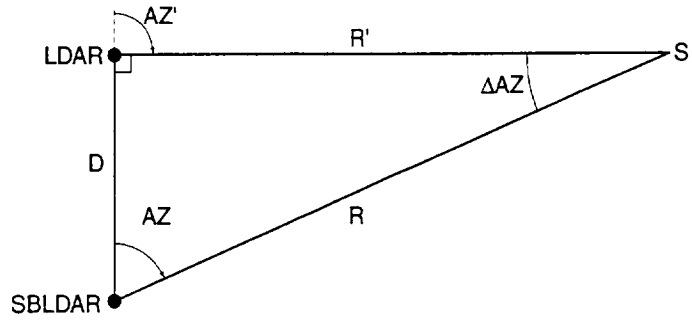

Figure 14. Geometry for SBLDAR AZ Correction to LDAR Coordinates

$$R \sin \Delta AZ = D \tag{75}$$

and for small ΔAZ

$$\Delta AZ = \frac{D}{R} \tag{76}$$

Because ΔAZ is a maximum when the source azimuth is perpendicular to $\overline{D}$, the function is modified with a sine function:

$$AZ' = AZ + \frac{D}{R} \cos\left(AZ + \tan^{-1}\left(\frac{Y_D}{X_D}\right)\right) \tag{77}$$

The origin of coordinate systems for the LDAR and the SBLDAR differ, so adjustments must be made to compare or mix the results from the two systems. For sources at an infinite distance, the AZ and EL seen from each system will be the same; however, for finite source distances, these corrections must be applied.

4. DATA ANALYSIS

4.1 DATA INTEGRITY

There are several useful approaches available to perform data and system integrity analysis. The most basic is to form additional channel-to-channel cross correlations and evaluate sums such as equation 78:

$$(T_0 - T_1) - (T_2 - T_1) - (T_0 - T_2) = 0 \tag{78}$$

This expression is not a tautology because the time differences are formed using the process of cross correlation and peak fitting. This approach does not work with a system such as LDAR, which simply identifies the peak value in the data record of each channel.

This formula was found to be very valuable during SBLDAR development because it characterized the total random timing errors in locating each lightning event. It is also useful in evaluating system repeatability when producing artificial RF pulses from a fixed location.

Unfortunately, this equation is not helpful in determining bias errors because each channel's fixed delays (K factors) also cancel.

Another useful relationship, valid only for the symmetrical, flat Y array is shown in equation 79:

$$(T_0 - T_1) + (T_0 - T_2) + (T_0 - T_3) \geq 0 \tag{79}$$

For sources at infinity, the equality holds. This can be seen by summing the equations in 17. For sources at finite range, each baseline contributes a positive residual so that the number is positive. During SBLDAR development, this equation was used as a quick data validity check. Sums that were negative were discarded. Also, events with large positive sums were discarded. All of these resulted from equipment failures and low signal levels (distant events).

This formula is also more useful than formula 78 because it does not entail additional cross correlations and because, for small residuals, it can produce a range estimate (see equation 62).

4.2 DATA TRIGGERING

Operation of the SBLDAR system depends on a system trigger (i.e., a command pulse directing the system to record and analyze data). Generally the hardware will be set up to record pretrigger data by using a continuous first-in-first-out (FIFO) data recording buffer. If the system is used in conjunction with LDAR to refine position estimates, the triggering scheme must ensure that the same pulse is analyzed on both systems. Using a pulse produced by a threshold trigger operated using the LDAR central site channel can ensure this because the SBLDAR is juxtapositioned with the LDAR (both places).

A moving trigger on the LDAR central channel (which has been proposed for an LDAR upgrade) presents a further difficulty but is still solvable by having a longer FIFO buffer. A moving trigger is one where potential events are identified but may be discarded in preference for a new one should a higher peak appear in a given time slot. Another proposed triggering scheme would trigger from any of the seven LDAR channels.

In the case of a simple real-time LDAR trigger, the SBLDAR FIFO need only be long enough to capture the data that occurs while the peak of the waveform traverses the SBLDAR array. In this system with 90-meter baselines, this would be the time required for light to traverse 180 meters plus signal on either side for about 650 nanoseconds. At a digitizing rate of 500 MHz (one data point per 2 nanoseconds), this is only 325 data points. A longer record may be desirable to ensure good correlation coherence (e.g., 512 points).

If any point in LDAR's 81.92 microsecond window could be chosen after the window closed, this recording requirement is increased to 40,960 data points per channel. However, if the windows are indefinite and the rate at which events are selected is high, then the FIFO size requirements can become extraordinary - not to mention the FIFO access time. An alternative could be to correlate data channels from each candidate peak rather than saving high data streams.

An entirely different approach to an integrated short- and long-baseline LDAR system is possible. Assuming the central antennas of each system are colocated and perhaps the same antenna, the SBLDAR system could just as well be used as the trigger. Thus, the SBLDAR system would identify events large enough to exceed a threshold, reliably estimate the direction (AZ, EL) of the source, and provide a rough estimate of range. Using the equations developed herein, an estimate of the location of the event record in the FIFO records from the long baselines could be quickly generated. This would facilitate either a rapid and efficient search of the long FIFO record or, even better, the more precise digitizing of the long baseline signals, only in the portion of the record of interest. This later approach would require long delay lines, so the SBLDAR processing is completed prior to the arrival of the earliest long-baseline pulse. This would potentially increase the time resolution on the long-baseline records and could eliminate completely incorrect event DTOA's (which is a common problem with the existing LDAR system).

The following discussion on data processing will not address the integration of short- and long-baseline LDAR because this issue is in a state of flux.

4.3 SBLDAR DATA PROCESSING

The flow of data processing should proceed generally as follows:

a. Receive trigger pulse (including time marker).

b. Continue to fill FIFO's for each channel to the specified level.

c. Read FIFO's in pairs into fast fourier transform processors that compute the cross correlation function. (The peak of this function is the best estimate of the time delay.)

d. Refine the time delay by performing a low order curve fit (i.e., third order) on an appropriately small number of points around the peak, then solve for the peak. (Alternatively, bond limited interpolation may be used for the curve fit.)

e. Subtract the bias delay differences (delta K's) from each delta T.

f. Evaluate the set of baseline delta T's for validity by performing a direct sum (which should be slightly positive).

g. Solve for AZ and EL for valid events.

h. Estimate the range for close events and refine estimates for AZ and EL (optional).

i. Clear trigger and reset FIFO for the next event.

5. CONCLUSIONS AND RECOMMENDATIONS

This report provides the results of analyses and algorithm development for an SBLDAR system. The analyses indicate that an equal arm Y-shaped array has very desirable properties because:

a. A single-step, least-squared-error algorithm can be used to rapidly and reliably estimate the AZ and EL of distant events.

b. The AZ error is independent of AZ.

c. The EL error is degraded compared to AZ but may be acceptable down to low elevation angles (near the mask angles of antennas).

d. The array can be easily augmented by a vertical baseline to capture EL data at low EL if necessary.

e. An iterative approach to solve for R, AZ, ΔEL for close-in events is available if required (see appendix A).

At the time of the development of this report, lightning data has been obtained by both the SBLDAR prototype system (described herein) and the LDAR system and acceptable agreement obtained. Full validation of the SBLDAR concept as an operational system has been completed.

Future work is anticipated to include additional SBLDAR data analysis with emphasis on increasing event processing speed. Also, integration of the SBLDAR into an overall LDAR system must be addressed. Both of these requirements will require the development, fabrication, and testing of state-of-the-art data capture and analysis hardware and software due to the high digitizing rate and rapid throughput (6,000 events per second) requirements. Future upgrades of LDAR may result in 30,000 events per second.

The work documented in this report is new. Carl Lennon developed the concept of using a short-baseline LDAR to correct the deficiencies of the existing LDAR system. Mike Brooks and Carl Lennon laid out the Y and vertical arrays. Stan Starr developed all the algorithms and formulas in this report and the concept of using the SBLDAR to trigger on events and find them on the long baselines. Mike Brooks and Bradley Burns developed

all the hardware and software in the prototype SBLDAR system. The exception to this is Geoff Rowe's work on the approach to cross correlating and peak fitting data records to estimate the time delays.

APPENDIX A

ITERATIVE SOLUTION FOR R, AZ, AND EL

When the source is relatively close to the array, significant errors in AZ and EL can result from the sensitivity of ΔT to R. In some applications of the algorithms, it may also be desirable to estimate R along with AZ and EL. This section derives a procedure for estimating all three variables.

Starting with equation 63, which approximates the measured delta T including the effects of curvature:

$$(T_i - T_0) = \frac{l}{c}\left(\cos EL_S \cos(AZ_S - AZ_{0i})\right) + \frac{l^2}{2cR}\left(1 - \cos^2 EL_s \cos^2\left(AZ_S - AZ_{0i}\right)\right) \quad (A1)$$

for a baseline lying in the EL = 0 plane.

It can be said, therefore, that ΔT is a function of AZ_s, El_s, R_s

$$\Delta T_{0i} = f\left(AZ_S, EL_S, R_S\right) \quad (A2)$$

If there is an approximate solution for these variables, the equation A1 can be used to compute an approximate ΔT_{2i} designated as $\overline{\Delta T}_{2i}$:

$$\overline{\Delta T}_{0i} = f\left(\overline{AZ}_S, \overline{EL}_S, \overline{R}_S\right) \quad (A3)$$

A procedure is needed for using the measured data (3 ΔT's) and the approximate AZ_s, EL_s, R_s to solve for the best AZ_s, EL_s, and R_s compatible with the data. If a Taylor expansion of AZ is taken using as a starting point the approximate solution, the equation A-4 is obtained.

$$\Delta T_{0i} = \overline{\Delta T}_{0i} + \left(AZ_s - \overline{AZ}_s\right)\frac{\partial f}{\partial AZ_s} + \left(EL_s - \overline{EL}_s\right)\frac{\partial f}{\partial EL_s} + \left(R_s - \overline{R}_s\right)\frac{\partial f}{\partial R_s} \quad (A4)$$

where all derivatives are evaluated at the estimated coordinates and only the first order terms have been retained. Evaluating each partial derivative:

$$\frac{\partial f}{\partial AZ_s} = \frac{-l}{c}\cos \overline{EL}_s \sin\left(\overline{AZ}_s - AZ_{0i}\right) + \frac{l^2}{cR_s}\cos^2 \overline{EL}_s \left(\cos\left(\overline{AZ}_s - AZ_{0i}\right)\sin\left(\overline{AZ}_s - AZ_{0i}\right)\right) \tag{A5}$$

$$\frac{\partial f}{\partial EL_s} = \frac{-l}{c}\sin EL_S \left(\cos\left(\overline{AZ}_s - AZ_{0i}\right)\right) + \frac{l^2}{CR_s}\cos \overline{EL}_s \sin\ \overline{EL}_s \left(\cos^2\left(\overline{AZ}_S - AZ_{0i}\right)\right) \tag{A6}$$

$$\frac{\partial f}{\partial R_s} = \frac{-l^2}{2CR_s^2}\left(1 - \cos^2 \overline{EL}_s \left(\cos^2\left(\overline{AZ}_s - AZ_{0i}\right)\right)\right) \tag{A7}$$

If the equation is labeled as:

$$\frac{\partial f}{\partial AZ_{0i}} = \alpha_{0i}, \quad \frac{\partial f}{\partial EL_{0i}} = \beta_{oi}, \quad \frac{\partial f}{\partial R_{0i}} = \gamma_{0i} \tag{A8}$$

then the Taylor expansion equations for all three baselines can be written as a matrix equation:

$$\begin{pmatrix} \Delta T_{01} - \overline{\Delta T}_{01} \\ \Delta T_{02} - \overline{\Delta T}_{02} \\ \Delta T_{03} - \overline{\Delta T}_{03} \end{pmatrix} = \begin{pmatrix} \alpha_{01} & \beta_{01} & \gamma_{01} \\ \alpha_{02} & \beta_{02} & \gamma_{02} \\ \alpha_{03} & \beta_{03} & \gamma_{03} \end{pmatrix} \begin{pmatrix} AZ_S - \overline{AZ}_S \\ EL_S - \overline{EL}_S \\ R_S - \overline{R}_S \end{pmatrix} \tag{A9}$$

For this equation to be solvable, the determinant of the derivatives matrix must exist (be nonzero). Although complicated, it can be shown that the solution exists. It should be noted, however, that as R increases, the size of the γ terms rapidly decrease, which decreases the numerical stability of the scheme.

The solution approach could be to: solve for AZ and EL using the algorithm given in section 2.4; then estimate the range using equation 62; compute the $\overline{\Delta T}$'s using equation 63; next, compute the residuals matrix of the $\Delta T - \overline{\Delta T}$ terms; solve for each of the terms in the derivatives matrix; and invert the derivatives matrix and apply it to the residuals matrix. This will give the matrix of corrections to the estimated AZ, EL, and R coordinates. These corrections are applied to the original estimates to derive a new set. This process is repeated until the residuals matrix becomes very small or zero.

APPENDIX B

REFERENCES

1. Godfrey, R., Mathews, E.R., and McDivitt, J.A., "Analysis of Apollo 12 Lightning Incident," MSC-01540, February 1970.

2. Uman, Martin A., "Electrical Breakdown in the Apollo 12/Saturn V First Stage Exhaust," Westinghouse Research Laboratories, Research Report 70-9C8-HIVOL-R1. May 4, 1970.

3. Brooks, M., Holmes, C.R., and Moore, C.B., Lightning and Rockets: Some Implications of the Apollo 12 Lightning Event, New Mexico Institute of Mining and Technology, Socorro, New Mexico.

4. Durrett, W.R., Lightning - Apollo to Shuttle, Thirteenth Space Congress Proceedings, April 7-9, 1976.

5. Christian, H.J., Crouch, K., Fisher, B., Mazur, V., and Perala, R.A., The Atlas-Centaur 67 Incident, Document ID: 19880035060 A (88A22287), Report Number: AIAA Paper 88-0389, January 01, 1988.

6. Kennedy Space Center Safety Practices Handbook, KHB 1710.2C, February 27, 1997.

7. Lennon, C., and Maier, L., Lightning Mapping System, NASA Conference Publication 3106, Vol. II, John F. Kennedy Space Center, 1991 International Aerospace and Ground Conference on Lightning and Static Electricity, Cocoa Beach, Florida, April 16-19, 1991.

8. Lightning Detection and Ranging (LDAR) System Certification Document, NASA and NYMA, Inc., Under NASA Contract NAS10-11835, September 14, 1994.

9. Godara, Lal C., IEEE, Application of Antenna Arrays to Mobile Communications, Part II: Beam-Forming and Direction-of-Arrival Considerations, Proceedings of the IEEE, Vol. 85, No. 8, August 1997.

10. Jenkins, Herndon H., Small-Aperture Radio Direction-Finding, Artech House, Inc., Boston:1991.

11. Mazur, Vladislav, Williams, Earle, Boldi, Robert, Maier, Launa, and Proctor David E., "Initial Comparison of Lightning Mapping With Operational Time-Of-Arrival and Interferometric Systems, Journal of Geophysical Research, Vol. 102, No. D10, Pages 11,071-11,085, May 27, 1997.

12. Mazur, Vladislav, Williams, Earle, Boldi, Robert, Maier, Launa, and Proctor, David E., "Comparison of Lightning Mapping With Operational Time-Of-Arrival and Interferometric Systems," NAWCADPAX—95306-PRO, Proceedings of the 1995 International Aerospace and Ground Conference on Lightning and Static Electricity, Williamsburg, Virginia, September 26-28, 1995.

13. Rhodes, C.T., Shao, X.M., Krehbiel, P.R., and Thomas, R., "Observations of Lightning Processes Using VHF Radio Interferometry," NASA Conference Publication 3106, Vol. II, 1991 International Aerospace and Ground Conference on Lightning and Static Electricity, Cocoa Beach, Florida, April 16-19, 1991.

14. Lee, Harry B., "A Novel Procedure for Assessing the Accuracy of Hyperbolic Multilateration Systems," IEEE Transactions on Aerospace and Electronic Systems, Vol. AES-11, No. 1, January 1975.

15. Torrieri, Don J., "Statistical Theory of Passive Location Systems," IEEE Transactions on Aerospace and Electronic Systems, Vol. AES-20, No. 2, March 1984.

16. Poehler, Horst A., Ph.D., "Error Analysis of Y-Configured Hyperbolic and Alternative Systems," RCA 620-5006, January 23, 1979.

17. Poehler, Horst A., Ph.D., "An Accuracy Analysis of the LDAR System," NASA Contractor Report CR-154631, Federal Electric Corporation, FEC-7146, 8 March 1977.

18. Cannon, John R., Ph.D. and Lennon, Carl L., "A Study of Various Methods for Calculating Locations of Lightning Events," 1995 NASA/ASEE Summer Faculty Fellowship Program, John F. Kennedy Space Center, University of Central Florida, August 22, 1995.

19. Cannon, John R., Ph.D., and Pyle, Bradford A., "A Study of the Geometric Dilution of Precision (GDOP) for the Lightning Detection and Ranging System (LDAR) and Methods of Solution Compensating for GDOP," 1996 NASA/Graduate Student Researchers Program, John F. Kennedy Space Center, University of Central Florida, December 12, 1996.

20. Thomson, E.M., Medelius, P.J., and Davis, S., "System for Locating the Sources of Wideband dE/dt from Lightning," Journal of Geophysical Research, Vol. 99, No. D11, Pages 22, 793-22, 802, November 20, 1994.

21. Uman, Martin A., The Lightning Discharge, Academic Press, Inc., Harcourt Brace Jovanovich, Orlando:1987.

22. Shelby, S.M. Ed., Standard Mathematical Tables, 21st Ed., Chemical Rubber Co., Cleveland, OH, 1973.

REPORT DOCUMENTATION PAGE

Form Approved
OMB No. 0704-0188

1. AGENCY USE ONLY *(Leave blank)*	2. REPORT DATE	3. REPORT TYPE AND DATES COVERED
	August 1998	Technical Memorandum - 1998

4. TITLE AND SUBTITLE
Development of Algorithms and Error Analyses for the Short Baseline Lightning Detection and Ranging System

5. FUNDING NUMBERS

6. AUTHOR(S)
Stanley O. Starr, Dynacs Engineering, Inc., Kennedy Space Center

7. PERFORMING ORGANIZATION NAME(S) AND ADDRESS(ES)
NASA John F. Kennedy Space Center
Kennedy Space Center, Florida 32899

8. PERFORMING ORGANIZATION REPORT NUMBER

9. SPONSORING / MONITORING AGENCY NAME(S) AND ADDRESS(ES)
National Aeronautics and Space Administration
Washington, D.C. 20546

10. SPONSORING / MONITORING AGENCY REPORT NUMBER
NASA TM-1998-207913

11. SUPPLEMENTARY NOTES

12a. DISTRIBUTION / AVAILABILITY STATEMENT
Unclassified - Unlimited
Subject Category:

This publication is available from the NASA Center for Aerospace Information, (301)621-0390

12b. DISTRIBUTION CODE

13. ABSTRACT *(Maximum 200 words)*

NASA, at the John F. Kennedy Space Center (KSC), developed and operates a unique high-precision lightning location system to provide lightning-related weather warnings. These warnings are used to stop lightning-sensitive operations such as space vehicle launches and ground operations where equipment and personnel are at risk. The data is provided to the Range Weather Operations (45th Weather Squadron, U.S. Air Force) where it is used with other meteorological data to issue weather advisories and warnings for Cape Canaveral Air Station and KSC operations. This system, called Lightning Detection and Ranging (LDAR), provides users with a graphical display in three dimensions of 66 megahertz radio frequency events generated by lightning processes. The locations of these events provide a sound basis for the prediction of lightning hazards. This document provides the basis for the design approach and data analysis for a system of radio frequency receivers to provide azimuth and elevation data for lightning pulses detected simultaneously by the LDAR system. The intent is for this direction-finding system to correct and augment the data provided by LDAR and, thereby, increase the rate of valid data and to correct or discard any invalid data. This document develops the necessary equations and algorithms, identifies sources of systematic errors and means to correct them, and analyzes the algorithms for random error. This data analysis approach is not found in the existing literature and was developed to facilitate the operation of this Short Baseline LDAR (SBLDAR). These algorithms may also be useful for other direction-finding systems using radio pulses or ultrasonic pulse data.

14. SUBJECT TERMS
Radio direction finding, lightning, arrays, error analyses

15. NUMBER OF PAGES

16. PRICE CODE

17. SECURITY CLASSIFICATION OF REPORT	18. SECURITY CLASSIFICATION OF THIS PAGE	19. SECURITY CLASSIFICATION OF ABSTRACT	20. LIMITATION OF ABSTRACT
Unclassified	Unclassified	Unclassified	